Mott phase in polarized two-component atomic Fermi lattice gas

M. Machida,[1,2,*] M. Okumura,[1,2,†] S. Yamada,[1,2,‡] T. Deguchi,[3,§] Y. Ohashi,[2,4,‖] and H. Matsumoto[2,5,6,¶]
[1]*CCSE, Japan Atomic Energy Agency, 6-9-3 Higashi-Ueno, Taito-ku, Tokyo 110-0015, Japan*
[2]*CREST, JST, 4-1-8 Honcho, Kawaguchi, Saitama 332-0012, Japan*
[3]*Department of Physics, Graduate School of Humanities and Sciences, Ochanomizu University, 2-1-1 Ohtsuka, Bunkyo-ku, Tokyo 112-8610, Japan*
[4]*Faculty of Science and Technology, Keio University, 3-14-1, Hiyoshi, Kohoku-ku, Yokohama, Kanagawa 223-0061, Japan*
[5]*Institute for Materials Research, Tohoku University, Katahira, Sendai 980-8577, Japan*
[6]*Department of Physics, Tohoku University, Aramaki, Aoba, Sendai 980-8578, Japan*
(Received 10 August 2008; revised manuscript received 4 November 2008; published 12 December 2008)

We investigate effects of pseudospin population imbalance on Mott phases in one-dimensional trapped two-component atomic Fermi gases loaded on optical lattices based on the repulsive Hubbard model in harmonic traps. By using the density-matrix renormalization-group method, we numerically calculate density profiles of each component and clarify the pseudospin magnetism. Consequently, we find that all the features from weakly imbalance to fully polarized cases are well described by $S=1/2$ antiferromagnetic Heisenberg chain under magnetic field. These results indicate that the Mott phases offer experimental stages for studying various interacting spin systems.

DOI: 10.1103/PhysRevB.78.235117 PACS number(s): 03.75.Ss, 71.10.Fd, 74.25.Jb, 74.81.−g

Recently, effects of population imbalance on interacting fermion systems have been intensively studied in various fields such as superconductors, atomic Fermi gases, and quantum chromodynamics.[1] The main reason is recent drastic developments of experimental techniques in superconductors and atomic Fermi gases.[2] In particular, in atomic Fermi gases, one can arbitrarily tune the population imbalance, so that not only the so-called Fulde-Ferrell and Larkin-Ovchinikov (FFLO) phase[3] with a spatially modulated superfluid order parameter but also the Chandrasekhar-Clogston limit[4] in a large imbalance has been explored.

In cold atomic gases, besides the tunable imbalance, the optical lattice and the variable interaction are like magic arts for condensed-matter physicists.[5] The optically created periodical potential flexibly builds up various playgrounds. The interaction tuning associated with the Feshbach resonance provides a chance to systematically study strongly correlated behaviors.[5] In this paper, we therefore study the population imbalance effect on the strongly correlated lattice stage, which is now one of the most intensive but controversial issues in solid-state matters.[6]

The atomic gas experiments usually employ the harmonic trap produced by magnetic field and/or optical method to avoid the escape of atoms. The harmonic trap brings about spatial inhomogeneities, which complicate the observation of the quantum phase transition.[7] Moreover, the fact that the most convenient probe is atomic density profile has limited the exploration of novel phases.[7] For example, the sign reversal in the FFLO superfluid order-parameter cannot be directly recognized by the density profile. Thus, the experimental confirmation of FFLO still remains controversial in the trapped system.[7,8]

On the other hand, the Mott insulator core accompanied by metallic wings predicted in the trapped optical lattice in the presence of the repulsive interaction[9] can be easily confirmed by the current probe like the density profile. These inhomogeneous phases have been proposed by quantum Monte Carlo studies[9] as well as the exact diagonalization method.[10] So far, theoretical studies of the Mott core phase have been restricted to a particular case, "balanced population." In this paper, we focus on the Mott phase in the presence of population imbalance. Using the density-matrix renormalization-group (DMRG) method,[11,12] we investigate pseudospin structures by calculating density profiles of each component in the Mott phase. Since the Mott core and its pseudospin structures are directly observable, their exploration will be a suitable next challenge in cold-atom physics.

Inside the Mott core, the on-site atomic density shows the unit filling and the density compressibility vanishes.[9] As a result, the pseudospin degree of freedom solely survives, so that the core region is well described by $S=1/2$ Heisenberg (local pseudospin interacting) model for the two-component atomic Fermi gas. Moreover, we expect that a population imbalance has a role of the magnetic field in the Heisenberg model given by

$$H_{\mathrm{eff}} = J\sum_{\langle i,j\rangle} \boldsymbol{S}_i \cdot \boldsymbol{S}_j - g\mu_B H_{\mathrm{ext}} \sum_i S_i^z, \tag{1}$$

where the fictitious magnetic field H_{ext} is varied by the magnitude of the population imbalance in the original system. In this paper, we explicitly confirm that the spin structure in the Mott core region is really described by the effective Hamiltonian (1) using the DMRG method.[11,12] Namely, we suggest that the Mott core can be employed as a model system to widely study the magnetism in interacting spin models. One of the advantages using the equivalence is that one can easily reach a very-high-field range. Moreover, although this paper concentrates on the one-dimensional and two-component Fermi atom system as a trial problem, higher-dimensional, frustrated, and large S cases are also possible to study.

The starting model Hamiltonian[9,10] describing trapped two-component Fermi atoms under the one-dimensional (1D) strong optical lattice is given by the 1D Hubbard model with the harmonic trap,

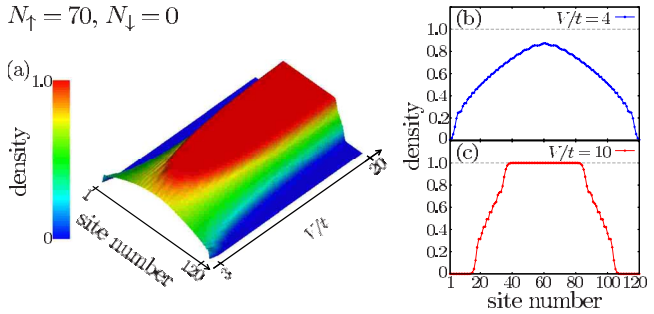

FIG. 1. (Color online) (a) The trap-potential strength V dependence of the particle density profile $n_{\mathrm{tot}}(i)[=n_\uparrow(i)]$ for a completely polarized fermionic gas with slice pictures for two cases (b) $V/t=4$ and (c) 10.

$$H_{\mathrm{Hubbard}} = -t\sum_{\langle i,j\rangle,\sigma}(c_{i\sigma}^\dagger c_{j\sigma} + \mathrm{H.c.}) + U\sum_i n_{i\uparrow}n_{i\downarrow} + V\left(\frac{2}{N-1}\right)^2\sum_{i,\sigma}\left(i - \frac{N+1}{2}\right)^2 n_{i\sigma}, \quad (2)$$

where the summation for the pseudospin σ is taken over two components assigned as $\sigma=\uparrow$ and $\downarrow$. $c_{i\sigma}^\dagger$ is the creation operator of a Fermi atom with the pseudospin σ at the ith lattice state and $n_{i\sigma}(\equiv c_{i\sigma}^\dagger c_{i\sigma})$ is the site density one for the same pseudospin. In the first term of Hamiltonian (2), t describes the nearest-neighbor hopping parameter and the summation $\langle i,j\rangle$ is taken over the nearest-neighbor sites, and U (>0) in the second term is the on-site repulsive interaction. The last term in Eq. (2) describes a harmonic trap potential, where V is the potential height at the edge sites. N is the total number of lattice sites and N_F is that of fermions with $\sigma=\uparrow$ and $\downarrow$ $(N_F \equiv N_\uparrow + N_\downarrow)$. Throughout this paper, an atom component with $\sigma=\uparrow$ is always a major one. As a main numerical method, we employ the DMRG to explore the ground state of model (2). At first, the number of states kept (m) in DMRG is selected by a comparison of the ground-state energy with the exact diagonalization method for small size $(N=20)$. In larger sizes, we select m which gives no significant difference by increasing m further. For $N=60(120)$ and 180(240) in the Hubbard model, we confirm that $m=100$ and $m=300$ are enough, respectively. In addition, for $N=60$ in the Heisenberg model, $m=100$ is selected due to the same reason.

Let us show DMRG results of model (2). First, we show atomic density profiles in the case of the perfect polarization $[P \equiv (N_\uparrow - N_\downarrow)/N = 1]$ in Fig. 1. When $V/t \gtrsim 5$, we find the insulating core in the center of the trap, over which the unit filling is spread. Since the compressibility is zero and the polarization is perfect in this insulating core, it is regarded as a ferromagnetic insulator. We note that this insulating state originates from only the Pauli exclusion principle and differs from the Mott state caused by a repulsive interaction between fermions. We also point out that this ferromagnetic insulating core can be described by the antiferromagnetic Heisenberg model (1) in the presence of a sufficiently strong magnetic field.

Next, let us study cases in which the minority-spin component slightly increases from zero (the complete polarized one). We examine density profiles in two typical situations, i.e., those in the presence of relatively weak and strong repulsive interactions. The upper and the lower panels in Fig. 2 are V/t dependences of density profiles of the former $(U/t=4)$ and the latter $(U/t=8)$ cases, respectively. As seen in Fig. 2, the unity core is broken in the central region about above $V/t=10$ in the weak-interaction case [Fig. 2(a)], while its flat plateau feature is still kept up to $V/t=20$ [Fig. 2(d)] in the strong-interaction one. Here, we note that the breakdown of the unity core is also observed above $V/t=20$ in the strong-interaction $(U/t=8)$ case. Namely, the V-dependent changes in the density profiles are qualitatively equivalent in both cases. On the other hand, we find from these results that the unity core is the so-called Mott state since its phase stability actually depends on the interaction strength.

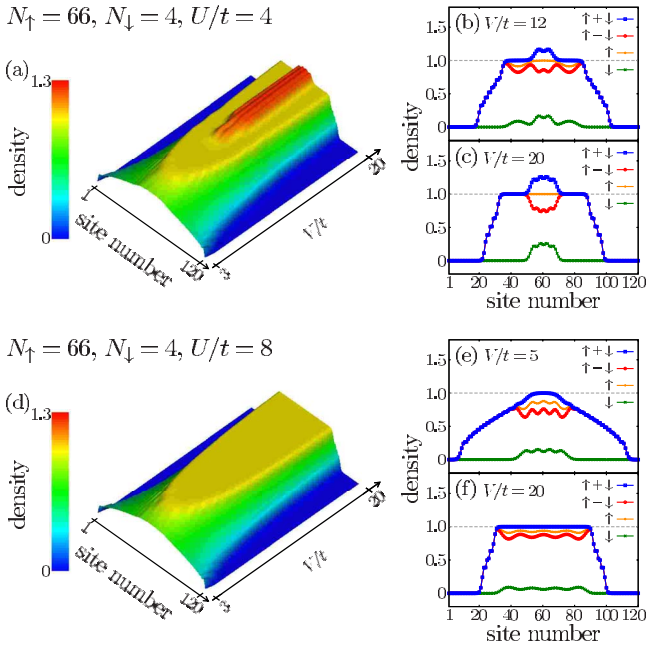

FIG. 2. (Color online) The trap-potential strength V dependences of the particle density profiles $n_{\mathrm{tot}}(i)[=n_\uparrow(i)+n_\downarrow(i)]$ for $N_\uparrow=66$ and $N_\downarrow=4$ in (a) $U/t=4$ with two slice pictures at (b) $V/t=12$ and (c) 20 and (d) $U/t=8$ with the same ones at (e) $V/t=12$ and (f) 20.

Now, let us concentrate on pseudospin structures inside the Mott phase as seen in Figs. 2(e) and 2(f). Before the Mott phase destruction occurs, we find that the minority makes a profile like Wigner lattice inside the Mott core. The number of the peak in the minority profile is the same as that of the minority atoms as seen in Figs. 2(e) and 2(f), where the number is just four [see Fig. 3(a) for another case in which the number is 10]. These Wigner-lattice-type profiles can be explained by the antiferromagnetic Heisenberg model (1) in finite but strong magnetic field. The effective model (1) then predicts the spin-density wave (SDW) state whose periodicity is characterized by $2k_F=\pi(1-\bar{m})$, where $\bar{m}$ is the magnetization normalized by the saturated magnetization and k_F is the Fermi wave vector in the equivalent spinless fermion system.[13] In the present imbalance system, since the $\bar{m}$ is a controllable parameter via the population imbalance, the periodicity is given by

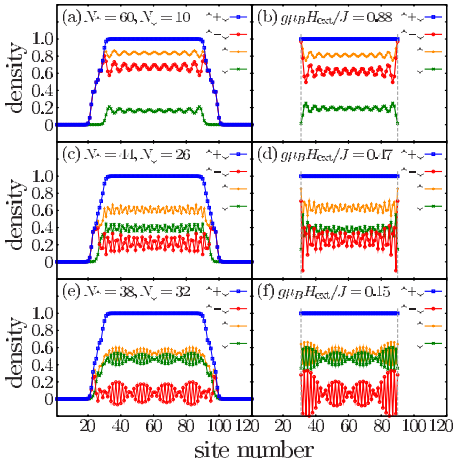

FIG. 3. (Color online) The profile changes in the Hubbard model (2) with decreasing the population imbalance ratio at $U/t=8$ and $V/t=20$. In the fixed total particle number $N_F=70$, (a) $N_\uparrow=60$, (c) 46, and (e) 38. The spin densities in the 60-site Heisenberg chain with the open boundary condition in the external magnetic field given by Eq. (1) are plotted with (b) $g\mu_B H_{ext}/J=0.90$, (d) 0.47, and (f) 0.15.

$$2k_F = \pi\left[1 - \left(\frac{N_\uparrow^{\mathrm{Mott}} - N_\downarrow^{\mathrm{Mott}}}{N^{\mathrm{Mott}}}\right)\right], \tag{3}$$

where $N_\uparrow^{\mathrm{Mott}}$ and $N_\downarrow^{\mathrm{Mott}}$ are the numbers of the up- and down-spin particles participating the Mott core, respectively, and N^{Mott} is the number of the lattice sites occupied by the Mott core. Thus, one finds why the minority profile shows Wigner-crystal-type ones, e.g., $2k_F=\pi[1-(56-4)/60]=2\pi\times 4/60$ in Fig. 2(f) and $2k_F=\pi[1-(50-10)/60]=2\pi\times 10/60$ in Fig. 3(a), where the Mott phase covers 60 sites ($N^{\mathrm{Mott}}=60$), $N_\uparrow^{\mathrm{Mott}}=N_\uparrow-10$ (ten majority particles contribute to make the metallic wings) and $N_\downarrow^{\mathrm{Mott}}=N_\downarrow$ as seen in Figs. 3(a) and 3(f). These profiles are really confirmed by the DMRG calculation of 60-site Heisenberg chain model in a magnetic field with the open boundary condition, e.g., compare Fig. 3(a) with Fig. 3(b). This result clearly demonstrates that the imbalanced Mott phases in the trapped Fermi lattice systems are equivalent with the effective interacting spin model under magnetic field.

Let us compare the spin-density distributions of the Mott core with ones of the Heisenberg model in more details. For this purpose, we evaluate the Fourier component $n_s(k)$ of the spin-density distributions $n_s(i)[=n_\uparrow(i)-n_\downarrow(i)]$ in a central range (from $i=31$ to 90, i.e., $L=60$) shown in Figs. 3(a) and 3(b). Figure 4 shows $k\equiv(\pi\ell)/(L+1)$ $(\ell=1,2,\ldots,L)$ vs $n_s(k)$. In these figures, one can find that a main peak characterizing the SDW structure (e.g., $\ell=21$) and other profiles almost coincide between both cases. This result indicates that the Mott phases confined inside the harmonic trap can be well described by the effective Heisenberg model with the open boundary condition.

We further decrease the population imbalance P, i.e., increase the number of the minority atoms. Then, the results, e.g., Fig. 3(c), reveal that the SDW periodicity is reduced according to $2k_F=\pi(1-\bar{m})$. We also note that by further imbalance decrease, in addition to the SDW spin configuration, another modulation structure with a wavelength being much longer than the lattice constant appears [see Fig. 3(e)]. This is regarded to emerge as a boundary effect since the incommensuration of $2k_F=\pi(1-\bar{m})$ with the lattice becomes visible, i.e., a beating modulation whose periodicity given by $\pi\bar{m}$ is exposed. For example, $2k_F=\pi[1-(33-27)/60]=\pi(1-6/60)$ in Fig. 3(e), where it is noted that both the majority (five particles) and the minority (five particles) equally contribute to the metallic wing. See another case, $2k_F=\pi[1-(31-29)/60]=\pi(1-2/60)$ in Fig. 5(f), where five majority and five minority particles also participate the metallic wing similar to Fig. 3(e). As shown in Figs. 3(d) and

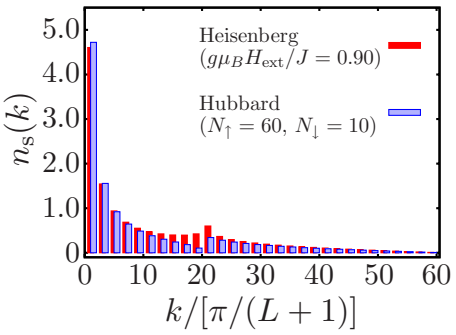

FIG. 4. (Color online) The comparison of k vs the Fourier-transformed spin density $n_s(k)$ for Figs. 3(a) and 3(b), i.e., the trapped Hubbard model (2) and the Heisenberg model (1) with the open boundary condition, in which $k\equiv(\pi\ell)/(L+1)$ $(\ell=1,2,\ldots)$, where $L=60$. In the case of the trapped Hubbard model, only the central core region is used for the Fourier transformation.

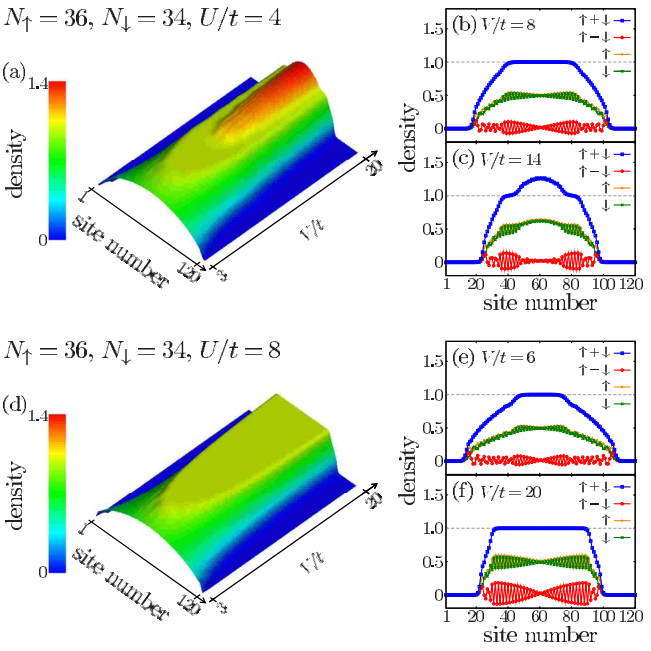

FIG. 5. (Color online) The trap-potential strength V dependences of profiles of the particle density $n_{tot}(i)[=n_\uparrow(i)+n_\downarrow(i)]$ for $N_\uparrow=36$ and $N_\downarrow=34$ in (a) $U/t=4$ with two slice pictures at (b) $V/t=12$ and (c) 20 and (d) $U/t=8$ with the same ones at (e) $V/t=12$ and (f) 20.

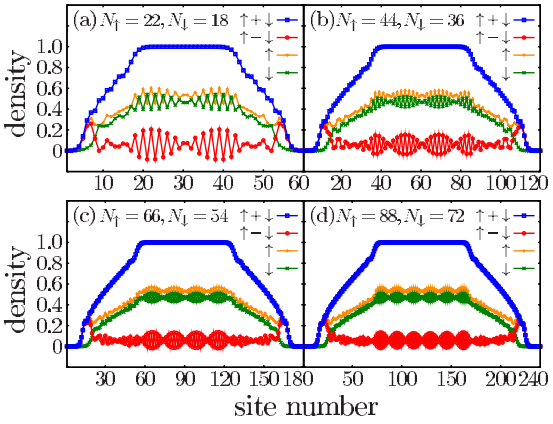

FIG. 6. (Color online) The site number N and the total atom number N_F dependences of the atom profiles with keeping the imbalance ratio for (a) $N_\uparrow=22$ and $N=60$, (b) $N_\uparrow=44$ and $N=120$, (c) $N_\uparrow=66$ and $N=180$, and (d) $N_\uparrow=88$ and $N=240$. In these cases, $U/t=20$ and $V/t=6$.

3(f), the change in the spin structure seen in Figs. 3(c) and 3(e) in Hubbard model (2) can be also well reproduced by decreasing the strength of the magnetic field in the effective model (1). One finds that even the beating modulation due to the boundary effect is also reproduced.

Let us turn to further small imbalance cases close to the balanced one. The upper and lower panels of Fig. 5 show V/t-dependent profiles in which the population ratio is 36:34 in strong and weak U/t, respectively. The profile in the weak interaction shows that the Mott insulator core is broken about above $V/t=12$ and the almost antiferromagnetic staggered profile is lost in the broken region as shown in Fig. 5(c). The loss of the staggered structure is also observed in the periphery[14] around the Mott core as seen in Fig. 5(b) [see Fig. 6(a) for another case]. These results clearly reflect that the staggered profile, i.e., the SDW phase, is formed only by the spin degree of freedom. The staggered profile diminishes in the metallic region in which the charge degree of freedom is alive. In addition, inside the Mott core, another long modulation is also observed in both the weak- and strong-interaction cases as seen in Figs. 5(b) and 5(f). In order to check the size dependence of this modulation, we examine the profiles by simply increasing both the lattice sites and the number of total atoms while keeping the population imbalance ratio a constant. The modulation and its wave periodicity are found to be almost size independent within the range as seen in Figs. 6(a)–6(d). These results indicate that such a modulation is clearly observable in 1D atomic Fermi gases loaded on optical lattices. In addition, we note that the effective Heisenberg model with the open boundary condition can reproduce these results.

We investigated the repulsively interacting polarized 1D Hubbard model with harmonic confinement potentials by using the DMRG method. Inside the core phase (where the site density equals to the unit) emerged universally for arbitrary P, we found that its spin structure is described by the antiferromagnetic Heisenberg model in magnetic field. This equivalence was confirmed by DMRG calculations for both the original and effective models. We suggest that the repulsively interacting polarized trapped lattice fermion systems offer various playgrounds of not only the Hubbard type but also the interacting localized-spin one. This idea may have an impact on studies of the magnetism in the solid-state physics.

One of the authors (M.M.) thanks T. Koyama, M. Kato, T. Ishida, H. Ebisawa, N. Hayashi, and T. Sakai for helpful discussions about superconductivity. The work was partially supported by Grant-in-Aid for Scientific Research on Priority Area "Physics of new quantum phases in superclean materials" (Grant No. 20029019) from the Ministry of Education, Culture, Sports, Science and Technology of Japan. This work was also supported by Grant-in-Aid for Scientific Research from MEXT-Japan (Grant No. 20500044). M.M. is supported by JSPS Core-to-Core Program-Strategic Research Networks, "Nanoscience and Engineering in Superconductivity (NES)."

*machida.masahiko@jaea.go.jp
†okumura.masahiko@jaea.go.jp
‡yamada.susumu@jaea.go.jp
§deguchi@phys.ocha.ac.jp
‖yohashi@rk.phys.keio.ac.jp
¶matumoto@ldp.phys.tohoku.ac.jp

[1] R. Casalbuoni and G. Nardulli, Rev. Mod. Phys. **76**, 263 (2004).
[2] See for reviews, e.g., I. Bloch, J. Dalibard, and W Zwerger, Rev. Mod. Phys. **80**, 885 (2008).; S. Giorgini, L. P. Pitaevskii, and S. Stringari, *ibid.* **80**, 1215 (2008), and references therein.
[3] P. Fulde and R. A. Ferrell, Phys. Rev. **135**, A550 (1964); A. I. Larkin and Y. N. Ovchinnikov, Sov. Phys. JETP **20**, 762 (1965).
[4] Y. Shin, C. H. Schunck, A. Schirotzek, and W. Ketterle, Nature (London) **451**, 689 (2008).
[5] For a review, see, e.g., M. Lewenstein, A. Sanpera, V. Ahufinger, B. Damski, A. Sen(De), and U. Sen, Adv. Phys. **56**, 243 (2007), and references therein.
[6] A. Bianchi, R. Movshovich, C. Capan, P. G. Pagliuso, and J. L. Sarrao, Phys. Rev. Lett. **91**, 187004 (2003); K. Kakuyanagi, M. Saitoh, K. Kumagai, S. Takashima, M. Nohara, H. Takagi, and Y. Matsuda, *ibid.* **94**, 047602 (2005); V. F. Correa, T. P. Murphy, C. Martin, K. M. Purcell, E. C. Palm, G. M. Schmiedeshoff, J. C. Cooley, and S. W. Tozer, *ibid.* **98**, 087001 (2007).
[7] For experiments, see, e.g., M. W. Zwierlein, A. Schirotzek, C. H. Schunck, and W. Ketterle, Science **311**, 492 (2006); G. B. Partridge, W. Li, R. I. Kamar, Y. Liao, and R. G. Hulet, *ibid.* **311**, 503 (2006); M. W. Zwierlein, C. H. Schunck, A. Schirotzek, and W. Ketterle, Nature (London) **442**, 54 (2006); Y. Shin, M. W. Zwierlein, C. H. Schunck, A. Schirotzek, and W. Ketterle, Phys. Rev. Lett. **97**, 030401 (2006); C. H. Schunck, Y. Shin, A. Schirotzek, M. W. Zwierlein, and W. Ketterle, Science **316**, 867

(2007).

[8] For theoretical works, see, e.g., A. Moreo and D. J. Scalapino, Phys. Rev. Lett. **98**, 216402 (2007); A. E. Feiguin and F. Heidrich-Meisner, Phys. Rev. B **76**, 220508(R) (2007); M. Tezuka and M. Ueda, Phys. Rev. Lett. **100**, 110403 (2008); G. G. Batrouni, M. H. Huntley, V. G. Rousseau, and R. T. Scalettar, *ibid.* **100**, 116405 (2008); M. Rizzi, M. Polini, M. A. Cazalilla, M. R. Bakhtiari, M. P. Tosi, and R. Fazio, Phys. Rev. B **77**, 245105 (2008); A. Lüscher, R. M. Noack, and A. M. Läuchli, Phys. Rev. A **78**, 013637 (2008); M. Casula, D. M. Ceperley, and E. J. Mueller, arXiv:0806.1747 (unpublished); A. E. Feiguin and F. Heidrich-Meisner, arXiv:0809.1539 (unpublished); A. E. Feiguin and D. A. Huse, arXiv:0809.3024 (unpublished).

[9] M. Rigol and A. Muramatsu, Phys. Rev. A **69**, 053612 (2004).

[10] M. Machida, S. Yamada, Y. Ohashi, and H. Matsumoto, Phys. Rev. Lett. **93**, 200402 (2004).

[11] S. R. White, Phys. Rev. Lett. **69**, 2863 (1992); Phys. Rev. B **48**, 10345 (1993).

[12] For recent reviews, see, e.g., U. Schollwöck, Rev. Mod. Phys. **77**, 259 (2005); K. A. Hallberg, Adv. Phys. **55**, 477 (2006), and references therein.

[13] T. Giamarchi, *Quantum Physics in One Dimension* (Oxford University Press, New York, 2004).

[14] In the metallic peripheries in Figs. 5(b), 5(c), and 5(e), antiferromagneticlike zigzag configurations are found, but the periodicities are larger than the lattice constant.